ILLINOIS STATE WATER SURVEY

at the

University of Illinois

Urbana, Illinois

RHI RADAR-HAIL RELATIONS FOR WEATHER MODIFICATION EXPERIMENTS

by

Stanley A. Changnon, Jr., and Donald W. Staggs

FINAL REPORT

National Science Foundation
Atmospheric Sciences Section
NSF GA-4618

July 16, 1970

TABLE OF CONTENTS

INTRODUCTION

The potential of radar data in the operational phases of cloud seeding projects, in research concerning hail physics, and as a single-instrument source of surface hail occurrence data makes it imperative that thorough investigations of radar-hail relations be pursued. Previous radar-hail investigations (Wilk, 1961) have not provided results that can be used to evaluate adequately radar as a detector of surface hail. The Russian hailstorm seeding activities (Sulakvelidze, 1966) have been anchored to the operational use of radar to detect storms for seeding and to study changes produced in radar echoes after seeding. The possibility that radar could also provide a measure of all hailstorms (the number and areal extent over a seeded area) is of equal importance in many potential seeding areas where the collection of surface hail data is very difficult or impossible (Rinehart and Staggs, 1968).

The research project described in this report was an outgrowth of an earlier Water Survey hail research program. The four major phases of the Illinois hail research have been:

1. Analyses of various historical hail data to determine the most meaningful statistical seeding designs and methods of evaluation.

2. Studies of various past and recent surface hail data collected in Illinois to provide basic statistics on hailstorm characteristics.

3. Development of a recording hailgage and passive hail instruments that would provide objective measures of hailfall intensity for employment in hail study areas.

4. Radar-hail investigations to determine the capability of radars to detect storms producing hail.

The last two phases were pointed toward a problem inherent in potential hail modification projects in many areas. That is, existing data, which are mostly hail-days data for a few discrete points or crop-loss data from insurance records, are often not adequate in historical length, areal coverage, or objectivity to monitor the results of seeding projects (Changnon, 1969). Thus, other reliable means of providing meaningful hail data are needed.

This particular research project, NSF GA-4618, concerned radar-hail investigations involving a specially modified RHI (TPS-10) radar and a nearby dense surface hail network within a 1000-square-mile area. This work was proposed because of the RHI-hail results for one hail day in September 1967 proved that more useful information on the detectability of hailstorms (and non-hailstorms) and on the physics of hailstorms could be gained from the almost instantaneous echo intensity information collected by rapid radar scanning over

a restricted sector (Staggs, 1968). The radar location and the hail network employed in this particular project are shown in Figure 1.

The two major goals of this specific research project were: l) to study further the detection of hail by radar using an RHI system specially modified and operated in a mode to present 3-dimensional and 8-reflectivity level portrayals of all echoes over and around a 1000-square-mile hail network, and 2) to develop an analytical system involving echo digitization and computer processing to handle and reduce the immense volume of radar data generated by the system and its mode of operation.

The TPS-10 3-cm radar has rapid vertical scanning that permitted relatively instantaneous vertical measurements of echo reflectivity. Further modification of the radar to increase the rate of data collection included use of sector scanning over the network, addition of iso-echo contouring, addition of a second receiver, addition of a second RHI scope, and the simultaneous photography of two RHI scopes with each displaying different reflectivity levels. The 1000-square-mile hail network could be scanned completely in 50 seconds with four gain-step (reflectivity) levels depicted. Four different (lower) gain levels were then automatically photographed in the next 50 seconds of the return sweep of the radar across the network sector. Thus, a complete 8 gain-step pictorial of all storms in three dimensions within the study area could be obtained in 100 seconds. However, with two photographs (one of each scope) made for every 2-degree (antenna beam width) sector, or once every second, this rapid scan and data acquisition rate yielded approximately 200 scope photographs per 100-second period.

Data reduction and analysis of such voluminous radar data plus the hail data collected during a few operational periods would be a virtually impossible task manually. Hence, the second aspect and goal of the project was to develop a technique to machine-process the radar and hail data. Development of such a technique would be necessary and invaluable aid in future real-time operations of a radar system for hail detection. In the technique developed, the filmed radar-scope data were translated into punch cards, using an OSCAR chart reading device to digitize the RHI data. These data plus the surface hail data on locations and times were then fed into the IBM 360-75 computer where much of the 2- and 3-dimensional echo analyses were performed. Such a data reduction and analytical process was found to be essential to handle and study the large volume of data that was produced from the rapid-cycling, iso-echo contouring of the radar echoes on three hail days. Although final analysis of all the RHI computerized data is not complete, the technique of computer analysis including programming has been completed.

In this report, selected results of an earlier CPS-9 radar-hail study are presented. The RHI radar analysis technique and selected results from the computer are presented plus results from a study of RHI echo bases and tops from a major hail day. Subsequent sections describe personnel involved in the project and the reports and publications derived from the research.

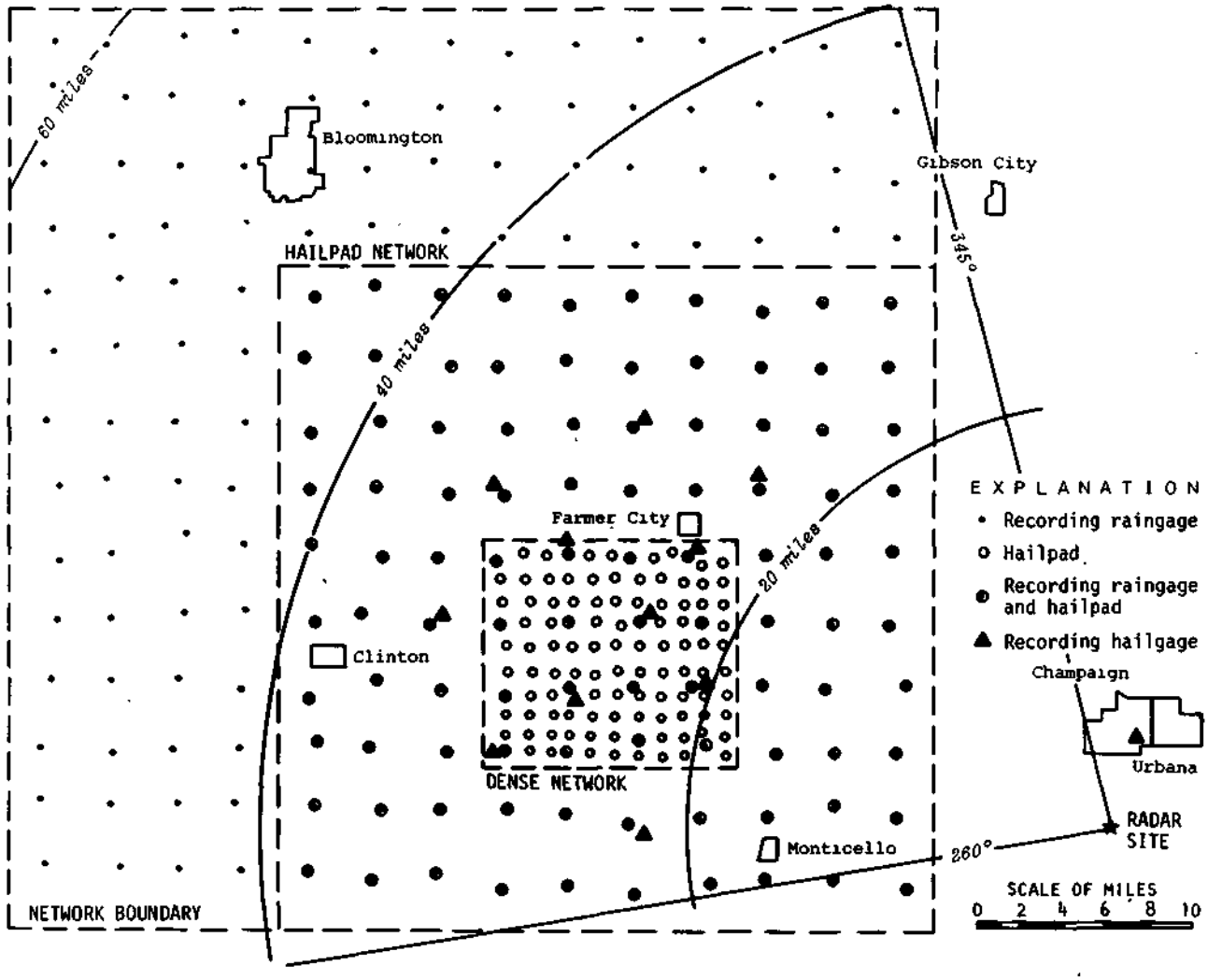

Figure 1. Radar site and hail network in Central Illinois.

OPERATIONS AND DATA

The plan of the project called for a collection of radar and hail data during the May-September period of 1968, followed by a 6- to 12-month period of analysis. The hail network was put into operation in May 1968, but the rebuilding and modification of the TPS-10 radar to provide the two scopes and related electronic features desired for the special operations were not completed until late August 1968. This delay plus the lack of hail occurrences in September 1968 required a second operational season in 1969 to secure data reasonably adequate to reach the goals of this project. However, this delay increased the length of the project approximately one year over that planned.

The hail study area included 196 recording raingages located in a 1600-square-mile area. Each gage had been modified to record the occurrence of hail as well as that of rainfall so that the rain characteristics occurring with hail could be studied. Secondly, 260 farmers in this 1600-square-mile area were volunteer hail observers, each being furnished detailed reporting cards to complete and mail upon the occurrence of hail. Several observers were also telephone reporters of hail. Hail data also came from all the crop-hail insurance companies in the network area, each of whom supplied detailed adjustor loss worksheets for all damaging storm days. Within the average network area, a 1000-square-mile hail network area was established with a hailpad installed at each of the 100 raingages, as denoted in Figure 1. A dense hailpad network was installed within this 1000-square-mile hail network with a hailpad for each square mile forming a 10-by-10 mile square (Fig. 1). A further data collection facility was installed in the network during 1969 when 13 recording hailgages were installed and operated. Hail network operations were performed from May through September in 1968, and from April through October 1969.

Radar operations occurred on 71 days within the September 1968 and the late May-early October 1969 periods. Radar echoes were sufficiently convective in nature to require scope camera operations on 50 of the 71 operational days (Table 1). Camera operations on the two RHI scopes occurred on 109.2 hours, and resulted in a combined total of 21,000 feet of 16-mm film. The number of days with useful data and non-useful data during the radar operational periods of 1968 and 1969 are shown in Table 1. Of the eight hail days on the network, only three had data that could be classified as useful. Of the other five hail days, two had non-useful data because of equipment failures, one because of non-radar operations (hail between 0330 and 0420), and two because the hail did not fall at any instrument or location where the time of hail was accurately recorded. Detailed study of hail with rapid-cycling radar data requires very accurate hailfall data to position the hail carefully in space and time with respect to the echo. Thus, the delay of operations through most of the 1968 season was doubly unfortunate, since the major operational period of the radar system then occurred during the very low frequency hail season of 1969. Only seven hail days occurred in the 1000-square-mile network during the late May-early October 1969 period, whereas that same period included 18 hail days in 1968 and 15 hail days in 1967.

Table 1. Radar data collection periods in 1968-1969.

	Number of Days and Hours with Photographic Data		Number of Hail Days	
Month/Year	Days	Hours	Useful Data[1]	Non-Useful Data[1]
9/68	8	30.0	1	1
5/69	2	2.5	0	1
6/69	12	24.9	1	1
7/69	15	29.4	0	1
8/69	8	13.9	0	1
9/69	4	7.3	1	0
10/69	1	1.2	0	0
Totals	50	109.2	3	5

Useful data means that accurate temporal hail data were available plus satisfactory radar operations, and non-useful means one or both of the two data sources failed.

ANALYTICAL PROCEDURES

The echo data were converted from film to a digital format with the use of a Bensor-Lehner decimal converter (OSCAR) whose output was recorded on IBM cards. Complete intensity and time-coded coordinate information on all contour levels of each cycle were digitized. The technique gave a reproduction accuracy (machine and operator) of ± 500 feet in any dimension. The card output was then processed by the computer which generated "corrected data" tape (see Appendix). This corrected data tape defined a series of computer-assembled 3-dimensional echo maps with a range-corrected Z_e (mm^6m^{-3}) computed for each element of volume. Also incorporated in these tapes were the positions and times of hailfalls as obtained from the network data sources. These data tapes represented material ready for computer processing of their reflectivities and volumes. The statistics relating to the analytical digitization of the radar film data are presented in Table 2. All periods of hailfall on each day were digitized plus 10 to 30 minutes of echo data prior to the first surface hail. The data sample available for analysis includes six hail-producing echoes and three no-hail producing echoes. Several of the hail-producing echoes produced more than one hailstreak. The total amount of data digitized included 221 minutes of radar echo data, and this required 771 man-hours to digitize and 82,000 IBM cards. This data reduction approach, although time consuming and an analysis of only 2 percent of the scope photographs, required only 2 percent of the time that would have been needed by standard manual analyses.

Table 2. Statistics on the radar echo data digitized for computer study of hail and no-hail echo characteristics.

Date	Number of Echoes[1]		Operational Time Digitized		Analytical Aspects	
	Hail	No-Hail	Period, CDT	Total Minutes	Time Needed to Digitize, Hours	Cards Needed to Digitize Data
9/23/68	4	1	1026-1100 1147-1246	95	171	20,000
6/22/69	1	1	1613-1737	85	275	36,000
9/ 5/69	1	1	1525-1605	41	325	26,000
Total	6	3	-----	221	771	82,000

[1] An echo entity identified by a reflectivity contour of $Z_e = 10^3$ (mm^6m^{-3}).

For checking purposes and as an aid in studying the echo characteristics of hailstorms, plan-position maps of Z_e contours were drawn by a Calcomp plotter (Fig. 2) using the corrected data tape. These maps were plotted with a Z_e contour for each 1/2 order of magnitude of $Z_e \geqq 10^3$ (mm^6m^{-3}) and at each 2,000-ft elevation level for all radar cycles encompassing hail periods in the network. The four locations of hailfall existing in the 2-minute period represented in Figure 2 are shown by asterisk type symbols.

For each echo that produced hail at the ground and for selected no-hail echoes, the computer was used (see Appendix) to produce tables (for each 100-second radar sweep cycle) of areas of Z_e for each 1/2 order of magnitude of $Z_e \geqq 10^3$ mm^6m^{-3} at each 2,000-ft elevation, volumes of Z_e for each 1/2 order of magnitude of $Z_e \geqq 10^3$ mm^6m^{-3}, and the value and location of the maximum Z_e of each echo.

The centroid of the maximum Z_e contour at each 2,000-ft level in hail echoes was computed. From this point the change of reflectivity was calculated for each 1/2 mile on 45-, 90-, 135-, 180-, 225-, 270-, 315-, and 360-degree radials. These values, used in conjunction with the time of hail occurrence, were investigated for any characteristics that could be used to distinguish hail echoes from no-hail echoes.

RESULTS

CPS-9 Radar-Hail Echo Study

The Illinois investigations of radar-hail relationships in 1967 were largely concerned with reflectivity analyses of PPI data obtained with a CPS-9 3-cm radar system (Rinehart, Staggs, and Changnon, 1968). This study was

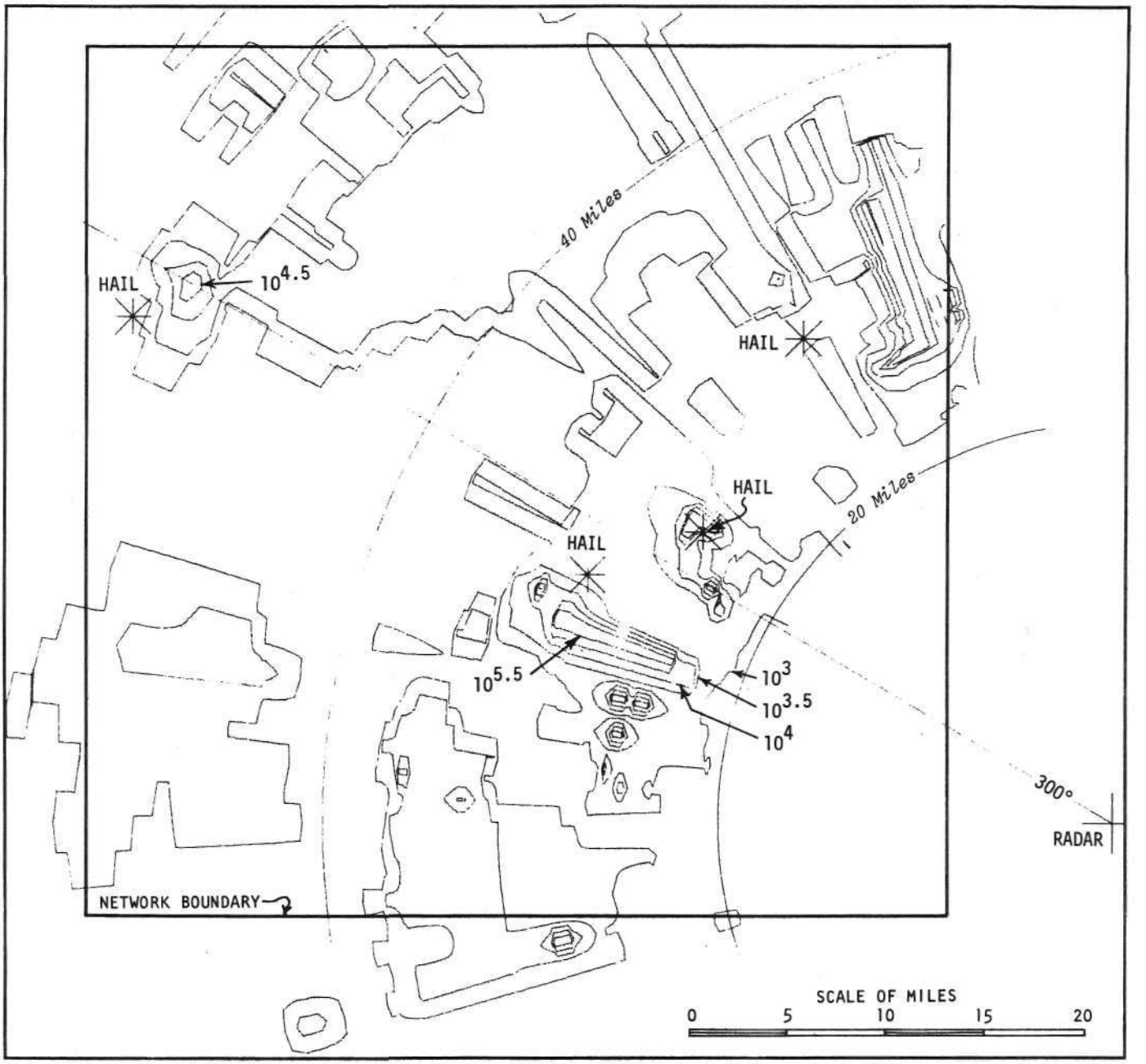

Figure 2. Calcomp plotted PPI from digitized RHI data for 23 September 1968 at 11:52:59-11:54:42 CDT. The altitude is 2,000 ft and reflectivity contours are for half-orders of magnitude (the outside contour is 10^3 mm^6m^{-3}).

performed as part of an earlier NSF grant (GA-482) and is described elsewhere (Changnon, 1969). However, a certain study of echo characteristics, as determined from the analysis of the PPI and available hail data, was completed and summarized under NSF GA-4618.

This later study provided results on various hail-echo characteristics including location, duration, direction of motion, speed, time of occurrence, reflectivity values, echo-top heights, and associated synoptic weather conditions for 103 hail-producing echoes. These results were compared with those obtained for 50 no-hail echoes. From these analyses, models of typical Illinois hailstorm echoes are developed, and results that have meaning for either hailstorm identification or hailstorm physics are identified and summarized.

The radar data consisted of PPI photographs taken in CPS-9 radar operations on .24 days during April-September 1967. The radar was operated with a maximum range of 80 nautical miles and with automatic sequential antenna-tilt and receiver gain reductions (gain step). A photograph was taken at each tilt angle and gain step. The surface reports of hail and no-hail came from a network of 1,380 cooperative hail observers and two smaller networks of 65 raingage-hailpad sites in an 18,000-square mile area encompassing central Illinois. These sources provided a total of 352 observer reports of hail time, 271 observer reports of no-hail, and 130 hail-time occurrences from the raingage-hailpad sites for the 24 days studied. Details on the analytical procedures and the many results can be found in a published paper (Towery and Changnon, 1970).

Results. Of prime importance were the facts that hail-producing echoes exhibited considerable variability in their durations, directions of motion, speeds, reflectivities, and heights. Figure 3 shows that echo tops at hail time had exceptional range (some as low as 9,000 ft and one as high as 54,000 ft at hail time), and, on the average, exhibited a surge of growth in the 10 minutes prior to hail. This suggests a strong convective surge during hail growth.

Several comparisons between the 50 hail-echo tops and the 50 no-hail echo tops, all of which formed within radar range, were made. Figure 4 is a real time average height graph depicting curves for hail and no-hail echoes as stratified by synoptic conditions. The average hail-echo tops were higher than those of the no-hail echoes in all but the earliest 20 minutes of stationary frontal echoes. The no-hail echoes exhibited very little growth after the 11-20 minute time interval, whereas the hail echoes almost always exhibited some increase after this interval.

Table 3 shows probabilities for different frequencies of taller echoes that will produce hail on any given hail day. Values indicate the possible confidence in predicting that tall echoes will be hailstorms. These probabilities are based on a comparison of the heights of the 50 hail echoes with those of the 50 no-hail echoes at formation, at average hail time (44 minutes after formation), and at dissipation. The taller half of the echoes on each day were used in this analysis. The probabilities at formation time show that on 38 percent of the days 81 percent or more of the taller echoes will become hailstorms, and that on 54 percent of the days more than 60 percent will become hailstorms. On 84 percent of the hail days, more than 60 percent of the taller half of the echoes

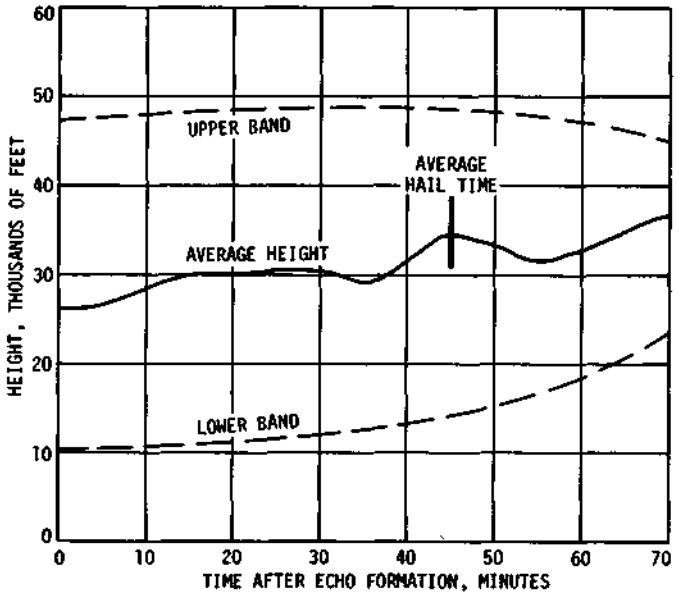

Figure 3. Average height curve and 90 percent envelope curves (made by upper and lower bands) for hail echoes for time after echo formation

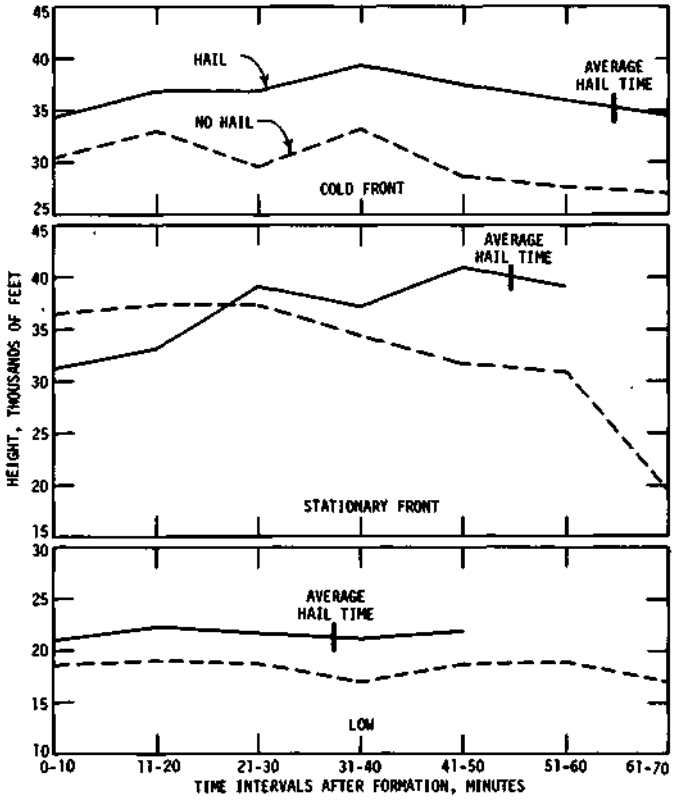

Figure 4. Height curves of hail and no-hail echoes for three major synoptic weather categories for time intervals after formation.

at hail time and at dissipation will be hailstorms. Since prediction at formation time is the most useful operational knowledge, it is important to realize that on 77 percent of the days more than half of the taller echoes at formation became hailstorms, and on 54 percent of the hail days more than 65 percent of the taller echoes became hailstorms.

Table 3. Daily probabilities that the tallest half of the echoes at different stages will produce hail.

Percent of tallest half of the echoes	Probability, percent, at different stages		
	Formation	Hail time*	Dissipation
81-100	38	46	54
61-80	16	38	30
41-60	23	8	16
21-40	23	8	0
0-20	0	0	0

*The heights used for analyzing no-hail echoes were those at the time corresponding to the average time of hail (44 minutes after formation), as based on all 50 hail echoes.

Analyses of the echo characteristics, when sorted and then grouped for the three principal synoptic weather categories, revealed distinctly different and reasonable models for each (Table 4). The hail-echo model for cold fronts is faster moving, as would be expected from the normal upper level steering winds with cold fronts, than are the other echo models. The cold frontal model also is the longest lived and highest storm (entire duration), and has relatively high reflectivities. The high reflectivity values also may relate to the fact that hail from cold frontal storms is relatively long lasting and that cold frontal hailstorms usually are associated with relatively heavy rainfall (Changnon, 1969).

The stationary frontal model of hail echoes indicates a right turn prior to the development of hail. Newton (1963) has indicated that severe storms embedded in warm moist air masses (which is the case for this condition) tend to obtain their indraft air at low levels along their southeast flank. Thus, new growth develops along the right flank which results in an apparent right turn in such an environment. The preference for afternoon echo development in the stationary frontal conditions further reflects the importance of low-level local heating on the development of hail echoes under this condition. The tendency for a left turn by hail echoes with cold fronts suggests that the heavier precipitation in these storms effectively blocks the primary upward inflow for the storm (Phillips, 1969). The primary flow circles inward on the left flank, which results in displacement of the updraft to the left and growth on the left flank in many cold frontal storms.

Table 4. Summary of echo characteristics for each synoptic classification.

	Cold front	Stationary front	Low
Average speed (kt)	30	21	25
Average duration prior to hail (min)	59	49	32
Average total duration (min)	90	83	75
Preferred direction of motion	NE	NE	ESE
Preferred direction of turn	Left	Right	No turn
Average number of degrees turn (when turning) in preferred direction	12	17	0
Preferred time of day, CST	1200-2400	1200-1800	0000-1800
Average reflectivity at formation (mm^6m^{-3})	5.6×10^2	5.1×10^2	4.6×10^2
Average reflectivity at hail time[1] (mm^6m^{-3})	2.6×10^5	4.6×10^5	5.2×10^4
Average reflectivity at dissipation (mm^6m^{-3})	3.5×10^3	9.1×102	2.6×10^3
Average top height for echo duration (10^3 ft)	38	36	19
Average top height at hail time[1] (10^3 ft)	37	38	20

[1]Hail time is the average time from echo inception until first hail.

The stationary frontal hail-echo model (Table 4) is shown by its reflectivity and height values to be a strong vigorous storm. This is not unexpected, because a large number of damaging Illinois hailstorms were produced under stationary frontal conditions.

The typical hailstorm produced by low conditions is the weakest and shortest lived of the three synoptic weather models. These storms exhibit a capability of producing hail fairly quickly after echo formation, but in turn the echo life is considerably shorter than those of the other models.

In general, the values in Table 4, which are considered to be models of Illinois hail echoes, appear to be reasonable because they are in agreement with prior findings on surface hail, instability with severe weather, and the mechanics of hailstorm development.

TPS-10 Radar-Echo Computer Analyses

Results for the eight echoes in the 221 minutes of digitized radar data are too exhaustive to allow a detailed presentation. All the digitized data have been completely processed to get "corrected data" tapes, and detailed final analysis is near completion for the echoes.

Selected results for two of the hail echoes are presented to illustrate the types of computer outputs being obtained and analyses thereof. One echo was one of a series of isolated small hailstorms on 23 September 1968 (Changnon, 1970), and the other was a large prefrontal echo that produced major hailstreaks on 22 June 1969.

The hail echo analyzed on 23 September (Fig. 2) was small in vertical extent (maximum top of 18,000 ft) and produced sparse hail ranging from 1/4 to 1/2 inch in diameter and three hailstreaks (ranging in length from 2 miles to 6 miles). In contrast, the hail echo on 22 June was large in vertical extent (tops to 44,000 ft) and produced two hailstreaks (one 3 miles in length and one 20 miles in length) with many stones ranging from 1/4 to 1-1/2 inches in diameter, the majority between 1/2 and 1 inch in diameter. The maximum rain rate at gages being affected by the hail echoes was 0.60 inch/hour on 23 September and 3.7 inch/hour on 22 June. The freezing level on both days was located at 12,000 ft.

Figure 5 shows selected Calcomp height-time plots of the 22 June echo for a 6.7-minute period. This figure adequately demonstrates the considerable variability of echo characteristics that occurs with time and altitude. For example, the areas of the 105.0 contour at 1710:38 at 12,000 and 24,000 ft are considerably different ($\approx$ 2.0 square miles at 12,000 as compared to $\approx$ 20 square miles at 24,000 ft). Also shown is the appearance of additional $10^{5.0}$ contours at 12,000 ft between 1710:38 and 1714:10 CDT. Hail was not falling at 1707, but hail was occurring at 1710, and a second hailfall area had appeared 3 miles to the southeast of the first by 1714. Comparison of the hailfall locations with their reflective plots at the different levels reveals that at the surface the hail areas are both near the forward edge where Z_e gradients are sharp, and that at both 1710 and 1714 the surface hailfall areas are positioned in or very

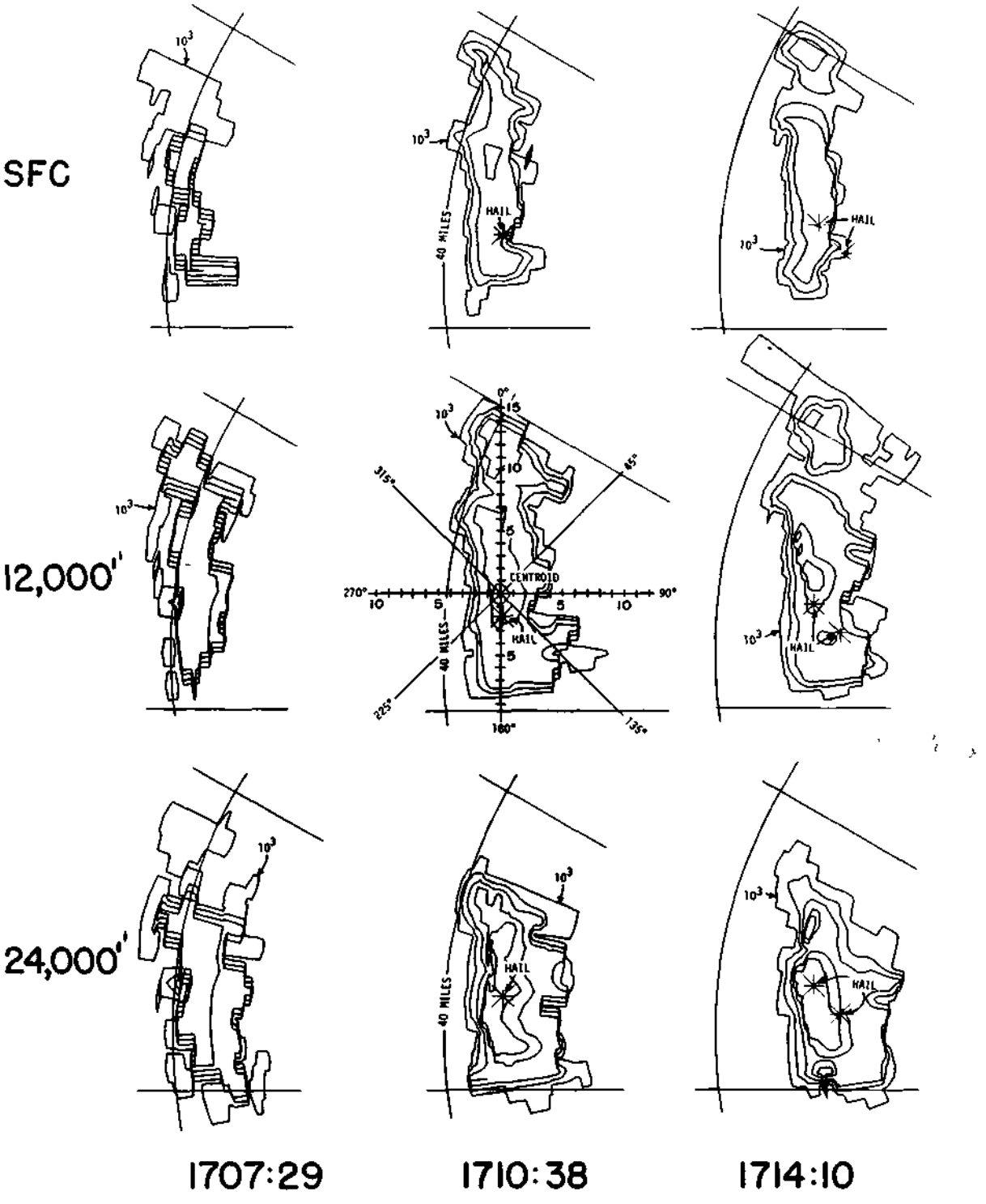

Figure 5. Computer generated CAPPI plots of Z_e (in half orders of magnitude for $Z_e \geq 10^3$) at depicted times and altitudes for 22 June 1969. The center outline shows an example of the radials used in the change of reflectivity analyses. The distance marks on the radials are spaced 1 mile apart.

close to the highest reflectivities shown at 12,000 and 24,000 ft. However, as also illustrated in Figure 5, hailfalls occur outside the areas of highest reflectivity.

The center outline (12,000 ft at 1710:38) was chosen to demonstrate some of the computer calculations of Z_e being performed at various locations within each echo being studied. These calculations are computed for points along each 45-degree radial drawn from the calculated centroid of the highest Z_e contour level. The results in Table 5 for the 0-degree, 135-degree, and 180-degree radials of this echo (Fig. 5 at 1710:38) reveal the echo extended beyond 6 miles. However, only the calculations for the first 6 miles from the centroid were shown. Values less than $10^{3.0}$ occur near the edge of echoes when the computer interpolates between the edge points and artificial zeroes used to terminate the calculations. In addition to the calculations of the Z_e at 1/2-mile intervals on radials, computer listings are made of the change in Z_e (in real numbers and in orders of magnitude) between the 1/2-mile points.

Table 5.- Z_e in the form "Log_{10} Z_e" at half-mile locations on the radials plotted on the center diagram of Figure 5. The origin of the radials is located at the centroid of the $10^{5.0}$ contour.

Distance from Centroid (mi)	Azimuth 0°	45°	90°	135°	180°	225°	270°	315°
0	5.469	5.469	5.1+69	5.469	5.469	5.469	5.469	5.469
0.5	5.139	5.065	5.110	5.122	5.237	5.247	5.383	5.276
1	4.809	4.752	4.816	4.859	5.001	4.773	4.486	4.616
1.5	4.647	4.547	4.610	4.680	4.808	4.452	4.266	4.514
2	4.671	4.502	4.484	4.554	4.653	4.334	3.815	4.479
2.5	4.706	4.469	4.420	4.452	4.505	4.146	1.306	4.279
3	4.701	4.436	1.614	2.696	4.499	3.937		3.919
3.5	4.706	4.199	1.782	3.268	4.494	3.652		3.438
4	4.695	3.675	1.022	3.673	4.486	3.336		0.156
4.5	4.621	2.990		3.800	4.476	0.649		
5	4.530	1.616		4.077	4.467			
5.5	4.503	0.376		4.334	4.473			
6	4.505			4.039	4.480			

Another example of the types of computer-produced results being obtained is revealed in Tables 6 and 7. These present the total volume of selected reflectivities and the number of distinct (spatially separate) hail occurrences for short periods of time during the lifetime of each hail echo. Comparison of the two tables illustrates intensity of the two hail echoes. For example, the maximum volume shown for the echo on 22 June (Table 6) was more than 1,000 cubic miles whereas the maximum volume on 23 September (Table 7) was approximately 430 cubic miles. Investigation of a higher reflectivity ($10^{4.0}$) reveals that

the maximum volume varies from 46 cubic miles on 23 September 1968 to almost 580 cubic miles on 22 June 1969.

Table 6. Volumes (mi^3) of specified reflectivities of the hail echo on 22 June 1969, time of occurrence, and the number of occurrences of surface hail at that time.

Time (CDT)	No. of Occurrences of Hail	Equivalent Radar Reflectivity $10^{3.0}$	$10^{3.5}$	$10^{4.0}$	$10^{4.5}$	$10^{5.0}$	$10^{5.5}$
1707:29	0	637.71	363.20	345.38	266.70	0.20	0.20
1709:05	1	977.02	715.85	541.28	271.07	50.02	27.83
1710:38	1	921.93	671.11	526.12	199.75	47.61	1.57
1712:17	2	1,005.96	696.61	535.74	179.30	62.88	
1714:10	2	953.05	618.19	482.76	116.28	51.36	
1715:55	1	1,038.71	720.56	578.15	137.21	77.94	

Table 7. Volumes (mi) of specified reflectivities of the hail echo on 23 September 1968, the time of occurrence, and the number of occurrences of surface hail at that time.

Time (CDT)	No. of Occurrences of Hail	Equivalent Radar Reflectivity $10^{3.0}$	$10^{3.5}$	$10^{4.0}$	$10^{4.5}$	$10^{5.0}$	$10^{5.5}$
1148:16	1	302.08	48.81				
1150:21	2	425.77	71.24	8.08	1.64		
1151:53	3	423.35	93.00	21.32	2.99	0.40	
1153:51	2	421.35	118.34	46.60	14.42	13.76	.08
1155:47	2	431.15	66.74	15.28			
1157:49	2	408:36	6.97				
1200:10	1	313.24	1.83				
1202:20	1	344.67	8.13				
1204.08	1	339.12	45.65	10.64			
1206:08	1	321.66	46.23	14.99			
1208:00	1	323.17					
1209:56	1	335.72	0.23				
1211:42	1	290.68	0.48				
1213:19	0	273.83	0.79				
1215:07	0	283.34	0.57				
1217:01	0	196.02					

Figure 6 is a plot based on the volumes of selected echo reflectivities located between 0 degrees C and -20 degrees C for both hail echoes. This figure allows a comparison of the volumes in the same temperature range and where hail formation was likely occurring. The top of the echo on 23 September did not reach the -20-degree C level. Also note that the abscissa scale is different for the two echoes.

The selected examples demonstrate a few of the many analyses that can be pursued at relatively low cost by computer processing of the quantified RHI radar data. Although the effect of attenuation is neglected and the data have limited signal integration, comparison of these two echoes at hail time illustrates the extreme variation in the sizes of hail echoes in Illinois and indicates the complexity of the problem of investigating radar characteristics of hail echoes. The' rapid changes in echo volume during periods of 5 minutes or less are also interesting results.

In addition to the hail reflectivity results, this analysis has proven that digitizing and computer-analyzing of radar data are desirable from the standpoint of reducing analysis time and cost. The equipment used in this analysis reduced the cost to one-tenth that of a comparable hand analysis. The logical extension of this analysis is to electronically scan and digitize the film or digitally record the radar data in computer format.

Even with the rapid cycling used to collect these data, there are some echo continuity problems in large unorganized storm systems which will make on-line computer analysis of these systems more complex than originally suspected.

Study of Temporal Variations in Echo Tops and Bases

The numerous echoes that occurred on the network on 22 June 1969 were selected for a special height-time study of the echo tops and bases. The previous research using PPI data indicated (Table 3 and Fig. 4) that hail-producing echoes were generally taller than no-hail echoes throughout their durations. The purpose of this particular echo top-base study was to check these earlier PPI results against those from the rapid scan RHI data.

During a 2-hour period (1613-1809 CDT) on 22 June, a total of 51 echoes formed over the network. During this period, seven hailstreaks occurred, but three of these were with echoes badly attenuated and not analyzed. Two echoes, each producing a single hailstreak, could be analyzed along with another echo that produced two large hailstreaks. The data sample included 53 other echoes that did not produce hail.

The bases and tops of each echo, as indicated on maximum radar sensitivity, were measured at the time of "first echo." First detection of particles sufficient in size and number to produce an echo was limited by the radar sampling frequency of 100 seconds. Thus, it is possible that some "first echoes" had been detectable for as much as 90 seconds before the radar scan sampled them. Bases and tops of each echo also were measured in every radar sweep (10 to 100 second) interval thereafter until the echo dissipated or moved too close to the

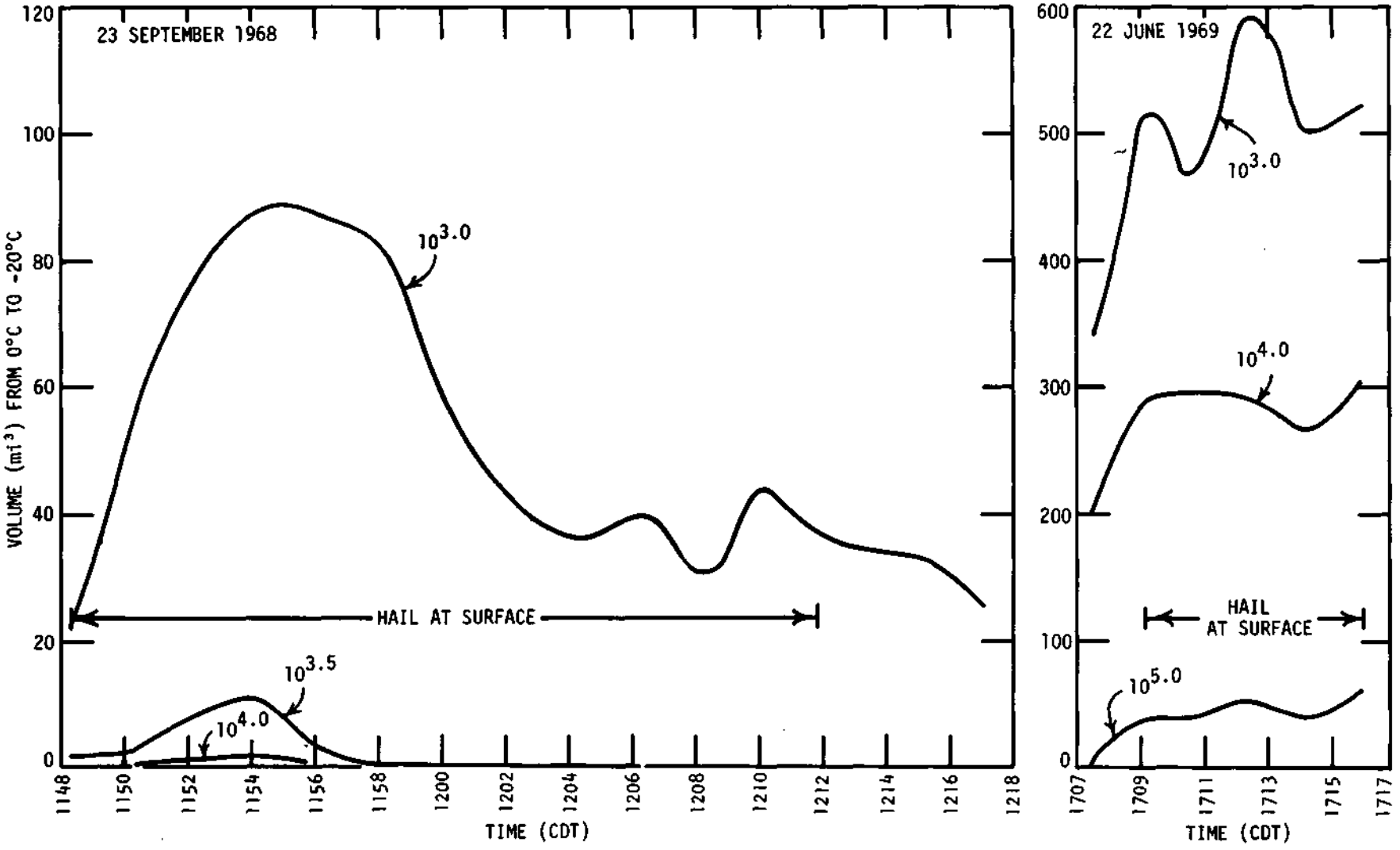

Figure 6. Echo volume (mi^3) from 0°C to -20°C of selected reflectivities plotted against time for 23 September 1968 and 22 June 1969. Hail is occurring at the surface during the indicated times.

radar for the top to be indicated. The echo-top measured was the highest point indicated. However, since the "tops" of several echoes had two or more turrets, the top value for such echoes was determined by averaging the heights of all turrets. The lowest point of the echo base (bottom) was the value measured and considered to be the echo base value.

No-Hail Echoes. The 48 no-hail echoes were sorted and classed into 5,000-ft height intervals based on the height of the top of the first echo. First echo tops occurred over a wide range, 13,500 to 28,000 feet, and four classes were developed beginning with the 10,000- to 15,000-ft interval. The number of echoes in each class is shown in Table 8. Average values for dimensions and times of the first echo, the maximum echo top stage, and the dissipation stage were calculated (Table 8), and the echo top characteristics for the echo durations were classified to derive models of the echoes in each class. The seven echo top characteristics discerned are listed in Table 9 along with the frequency of echoes for each characteristic listed according to each first echo top height class. Echoes in the two lower classes (10,000-15,000 and 15,000-20,000 ft) favored some growth followed by recession or leveling until dissipation. Most echo tops (15 of 23) in the 20,000- to 25,000-ft class were either level for 6 to 10 minutes followed by downward motion or were going downward continuously. Six of the eight echoes with first echo tops in the 25,000- to 30,000-ft class descended from the first echo height before becoming level 5 to 7 minutes after the first echo and remaining level until dissipation. The totals reveal that only 15 of the 48 no-hail echo tops had any upward motion.

The averages in preferred echo top characteristics were used to develop average profiles or models for each class (Fig. 7). The two lower formation classes were short lived, 5 and 8 minutes, respectively, from first echo to dissipation, and some had a short period of top growth. However, radar detectable particles never reached the ground in any of these 17 echoes. There were 23 echoes with first echo tops between 20,000 and 25,000 ft, making this class the largest. These echoes exhibited very little vertical growth, but lasted longer (28 minutes) than any other echo class. Echo bases in this class, and in the higher classes, reached the ground in 6 to 8 minutes after formation. Interestingly, the depths (top to base) of first echoes (Table 8) increased with the increasing height of echo class. For instance, the average depth of first echo in the lowest height class was 5,000 ft, whereas that for the first echo tops above 25,000 ft was 8,800 ft.

In general, these widely different no-hail echo classes revealed varying forms and degrees of convection. Analysis of their formation time shows that six of the eight largest echoes (> 25,000 ft) developed in the second hour of activity (1701-1800 CDT). Echoes with first echo tops in the 10,000- to 20,000-ft classes represented most of the echoes in the first half hour (1601-1630) of activity. After 1630 and until 1730 the occurrence of first echoes of varying sizes was randomly distributed with time.

Although the top and base characteristics of the taller (> 25,000-ft tops) first echoes differed somewhat, very few exhibited any growth after formation. Most of the no-hail echoes had durations of less than 20 minutes, and only three lasted 40 minutes.

Table 8. Average values for four classes of no-hail echoes on 22 June 1969.

Echo Class Based on Height of First Echo Top, Thousands of Feet	Number of Echoes	First Echo Dimensions (Thousands of Feet)			Time, Minutes, First Echo Base to Ground	Maximum Echo Stage		Dissipation Stage		
		Top	Base	Depth		Height, Thousands Ft	Time, Min, after First Echo	Height, Thousands Ft Top	Base	Time after First Echo, Min
10-15	3	14.0	9.0	5.0	---	16.0	2.0	13.7	8.0	5.0
15-20	14	17.9	10.7	7.2	---	20.3	4.5	18.0	6.0	8.0
20-25	23	22.6	14.2	8.4	8.5	23.0	6.0	15.0	0.0	28.0
25-30	8	26.2	17.4	8.8	6.5	26.2	0.0	20.0	0.0	23.0

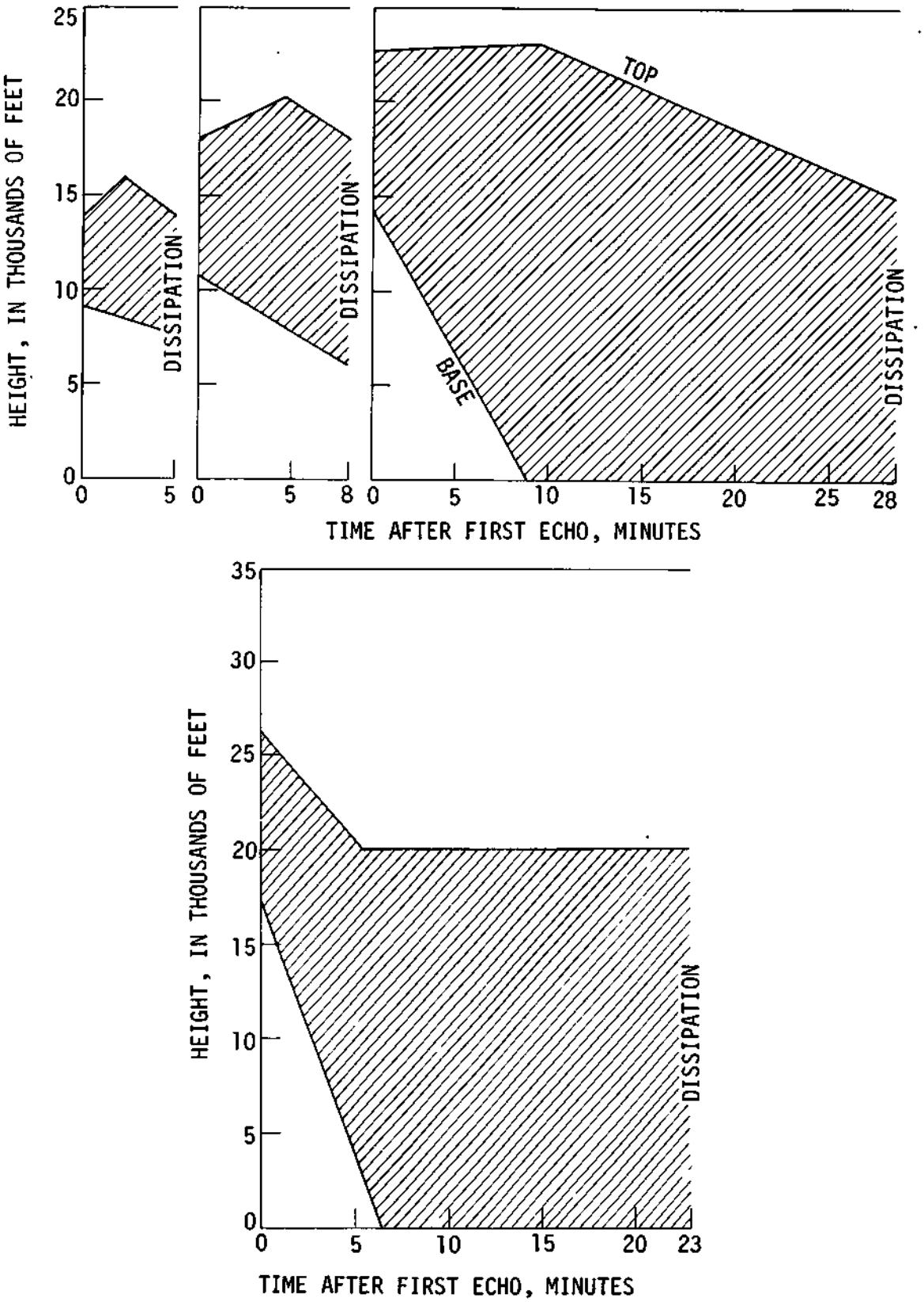

Figure 7. Average echo top-base profiles for different echo classes based on first echo tops on 22 June 1969.

Table 9. Frequency of no-hail echo top motion characteristics for different echo top classes.

Description of Echo Top Motion Characteristics	Number of Echoes in each 5,000-Ft Class, as Based on Top Height of First Echo				
	10-15	15-20	20-25	25-30	Total
Up then down, same rate	3	4	0	0	7
Up then level	0	3		10	4
Up rapidly then down slowly	0		12	1	4
Level	0	4	5	1	10
Down,	0	2	7	2	11
Level then down	0	0	8	0	8
Down then level	0	0	0	4	4

Hail Echoes. The profiles of the three hail-producing echoes on 22 June appear in Figure 8. The appropriate no-hail echo profiles, based on the height of the top of the first echo (hail), are also shown for each hail echo to examine for differences between hail and no-hail echoes. Also shown are durations for hailstreaks, including the 2 streaks of hail echo 2. The first conclusion is that first echo height alone is not a hail-echo distinguishing factor since 17 no-hail echoes had higher tops than hail echo 2, the highest of the three hail echoes. A second conclusion is that the three hail echoes were not alike in echo top behavior, duration, or stage when hail fell. Indeed, the three hail echoes aptly illustrate the considerable variability that exists in hail-producing storm echoes within a restricted time and area. Certainly, hail echo 2 (also illustrated in Figs. 5 and 6) is a major storm of great vertical development, areal size, and duration. However, hail echo 1 had only a slightly lower top (3,000 ft), but never evidenced any great vertical growth, and surface hail began 6 minutes after the first echo rather than 28 minutes (echo 2).

The three hail-producing echoes did exhibit certain characteristics that were not apparent in the 53 no-hail echoes. Comparison of the first echo depth (top to base) reveals that all three hail echoes had exceptionally greater depth at first detection, indicating a much greater volume of detectable particles to lower elevations within the cloud than did no-hail echoes. Consequently, the bases of the hail-producing echoes reached the ground much sooner than the model values. None of the no-hail echoes with tops forming in the 20,000-25,000-ft range had first echo depths as great as those with hail echoes 1 and 2, and the 9,500-ft depth on hail echo 3 exceeded any measured for the 15,000-20,000-echo top class.

Although hail echoes 1 and 3 did not exhibit exceptional vertical growth after formation, their maximum tops were 3,000 ft higher than their first echo. This difference is considerably more than that achieved by no-hail echoes in their classes (Table 8).

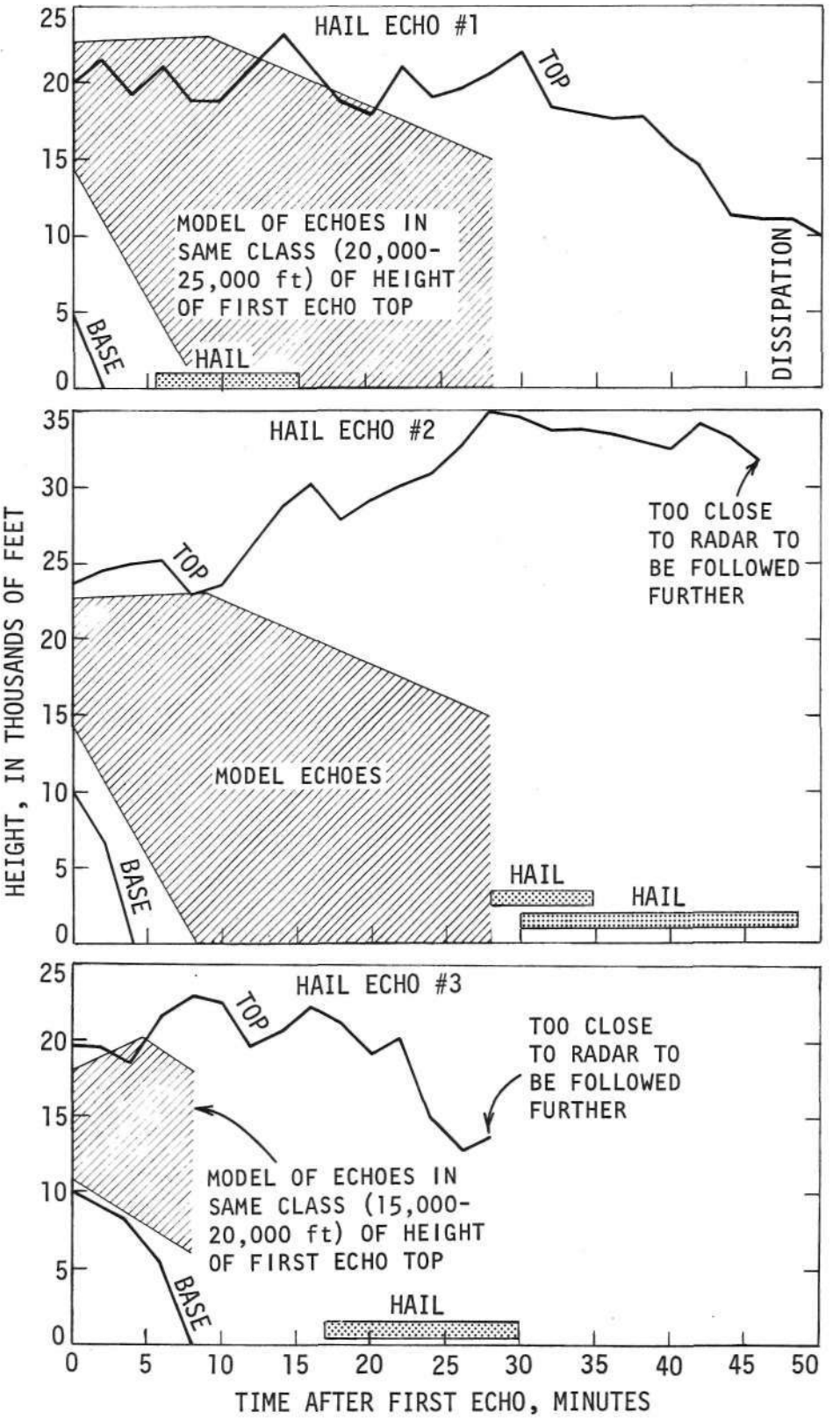

Figure 8. Profiles of three hai1-producing echoes on 22 June 1969.

Finally, the hail-producing echoes all had durations much greater than their associated models shown on Figure 8. Hail echoes 1 and 2 persisted longer than any no-hail echo on 22 June (although dissipation time of echo 2 was unknown), and hail echo 3 lasted at least 28 minutes which is longer than any of the 17 no-hail echoes that had first echo tops below 20,000 ft.

In conclusion, hailstorm detection by radar on 22 June could have been accomplished on three criteria:

1. Depths of first echoes for hailstorms were much greater than those for no-hail echoes.

2. Hail echoes exhibited greater growth than comparable (first echo) no-hail storms.

3. Hail echoes persisted much longer than no-hail echoes having comparable first echo tops.

PERSONNEL

During most of the project Neil G. Towery served as project radar meteorologist. He made significant contributions in all phases of the project including the radar operations, hail data analysis, and radar data analysis. He was preceded by Ronald E. Rinehart who capably assisted from August 1968 through April 1969.

The extensive and difficult computer programming required for this project was handled competently by Carl Lonnquist of the Survey staff. His interest and patience are greatly appreciated.

Mrs. Edna Anderson performed the routine cataloging and analysis of the hail network data, and servicing of the hail network was aptly handled by Daniel Watson and Eberhard Brieschke. Mr. Brieschke also aided Mrs. Phyllis Stone in the digitizing of the radar film data into punch cards. Mr. Joe Coons performed routine radar maintenance and calibrations.

Several student employees were involved in the research. Mr. Timothy Lewis, a graduate student in climatology at the University of Illinois, made a special study of RHI echo bases and tops. Mr. David Brunkow, an advanced undergraduate in electrical engineering, assisted in the radar servicing and in maintenance of the hail network equipment. Miss Deborah Hunt, an undergraduate in science education, worked on the collection and analysis of the hail network data.

PAPERS AND REPORTS

Published

1. Towery, N. T., and S. A. Changnon, 1970: Characteristics of Hail-Producing Radar Echoes in Illinois. Monthly Weather Review, 98, 346-353.

2. Towery, N. T., D. W. Staggs, and C. Lonnquist, 1970: Hailstorm Characteristics as Viewed by Rapid Scan RHI Radar. Preprints of Second National Conference on Weather Modification, Santa Barbara, 172-175.

3. Changnon, S. A., 1970: The Flail of the Lashing Hail. Computing Report, 6, 1.

Submitted for Publication

1. Changnon, S. A., 1970: Note on Hailstone Size Distributions. Journal of Applied Meteorology, 6 pp.

2. Changnon, S. A., and P. T. Schickedanz, 1970: Effect of Sensing Area Size on Hail Energy Calculations. Journal of Applied Meteorology, 8 pp.

In Preparation

1. Towery, N. T., D. W. Staggs, and S. A. Changnon, 1970: RHI Radar-Hail Detection Study. Proceedings 14th Weather Radar Conference, Tucson, 6 pp.

2. Staggs, D. W., and C. Lonnquist, 1970: Computer Analysis of Radar Weather Echo Data. Proceedings 14th Weather Radar Conference, Tucson, 6 pp.

In addition, two other published papers, although acknowledged to NSF GA-482, were partially based on data collected during GA-4618. These papers included:

1. Changnon, S. A., 1970: Hailstreaks. Journal of Atmospheric Sciences, 27, 109-125.

2. Changnon, S. A., 1970: Major Hailstorms Retrace Tri-State Tornado Track in Illinois. Transactions Illinois Academy of Science, 63, 34-41.

A national news release about the radar-hail research project was made in February 1970, and articles appeared in more than 100 newspapers. Some of the newspapers that carried the story included the "New York Times," "Chicago Tribune," and the "St. Louis Post-Dispatch."

REFERENCES

Changnon, S. A., 1969: Hail Evaluation Techniques. Part 1, Final Report NSF GA-482, Ill. State Water Survey, Urbana, 97 pp.

Changnon, S. A., 1970: Hailstreaks. Journal of Atmospheric Sciences, 27, 109-125.

Newton, C. W., 1963: Dynamics of Severe Convective Storms. Meteorological Monographs, 5, 33-58.

Phillips, B. B., 1969: Water Load in Convective Storms and Its Influence on Storm Kinetics. ESSA Technical Memorandum ERLTM-APCL 6, U. S. Department of Commerce, Applied Physics and Chemistry Laboratory, Boulder, Colo., 55 pp.

Rinehart, R. E., and D. W. Staggs, 1968: Use of Radar to Delineate Surface Hail Areas in Weather Modification Experiments. Proceedings National Conference on Weather Modification, 9 pp.

Rinehart, R. E., D. W. Staggs, and S. A. Changnon, 1968: Identification of Hail and No-Hail Echoes. Proceedings of the 13th Radar Meteorology Conference, McGill University, Montreal, August 20-23, 1968, American Meteorological Society, Boston, 422-427.

Staggs, D. W., 1968: RHI Gain-Reduction Studies of Hailstorms. Proceedings of the 13th Radar Meteorology Conference, 8 pp.

Sulakvelidze, G. K., 1966: Results of the Caucasus Anti-Hail Expedition of 1965. Trudy, 7, 1-61.

Towery, N. T., and S. A. Changnon, 1970: Characteristics of Hail-Producing Radar Echoes in Illinois. Monthly Weather Review, 98, 346-353.

Wilk, K. E., 1961: Radar Investigations of Illinois Hailstorms. Scientific Report No. 1, Contract No. AF19(604)-4940, Ill. State Water Survey, Urbana, 42 pp.

APPENDIX

Echo Card to Tape Program

The purpose of the echo card to tape program (see drawing) is to reconstruct the echo reflectivities from the digitized radar film. The digitized boundary for each radar sensitivity level is read from the cards and traced in an array with special characters. A scan of the array permits the labeling of all the interior points (1000-ft increments) within each contour.

Using the radar calibration, a minimum and maximum reflectivity is computed for each sensitivity level. A smooth reflectivity surface is generated using these limits. The reflectivities are then corrected for range and are ready to be stored on tape with their identification. The echoes stored on magnetic tape are in arrays representing vertical cross sections for every 2° of azimuth. Each array contains reflectivities at all 1000-ft increments from 15 to 60 miles in range and from 0 to 59,000 ft in altitude. The data are now in a format that permits many computer analyses, two of which are described below.

CAPPI Echo Plotting Program

The CAPPI echo plotting program (see drawing) prepares horizontal contoured cross sections of the radar echoes stored on tape. Plots are usually obtained for every 2000-ft level with reflectivity contour lines drawn at each half order of magnitude.

For each plot the required data are read from the echo tape and an array constructed which contains reflectivity values for every 2° azimuth and 1000-ft in range. This reflectivity array divides the echo map into small 4-sided areas as formed by adjacent range and azimuth lines. Each of these areas is examined to determine if a contour line passes thru it. If the four reflectivity values surrounding the area are in the same half order of magnitude range no line is present. When the surrounding values lie on both sides of a contour level of reflectivity, the location of the contour is interpolated from the reflectivity values, and the line segment contained in the area is plotted on the CALCOMP. The line segments from adjacent areas join to form complete contours.

In addition, locational information on any hail areas for the time of the CALCOMP plot is inserted and plotted.

Echo Volume - Gradient Analysis Program

The echo volume - gradient analysis program is used to calculate echo volume and reflectivity gradient statistics from the radar echo tapes (see drawing).

ECHO CARD TO TAPE PROGRAM

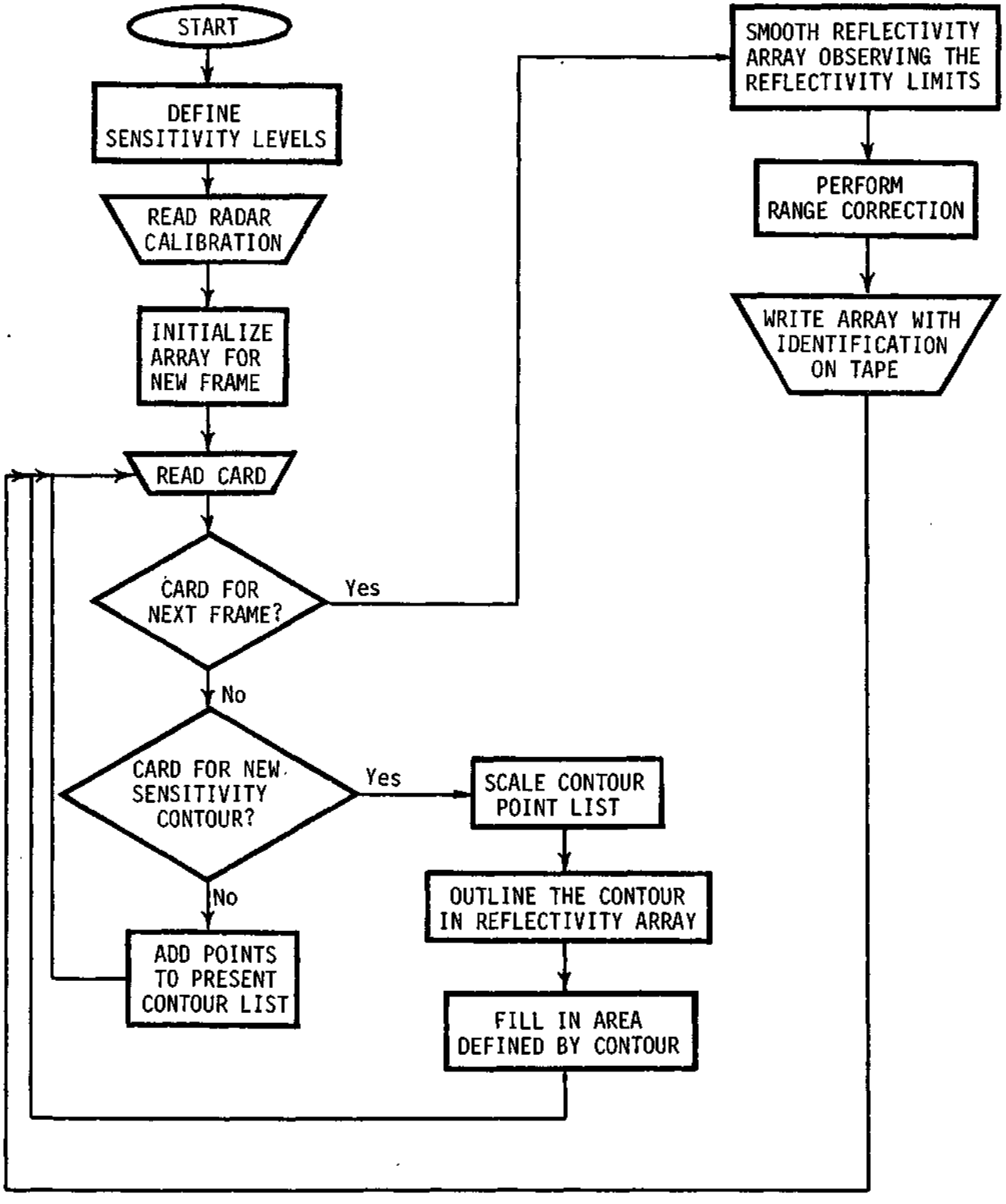

CAPPI ECHO PLOTTING PROGRAM

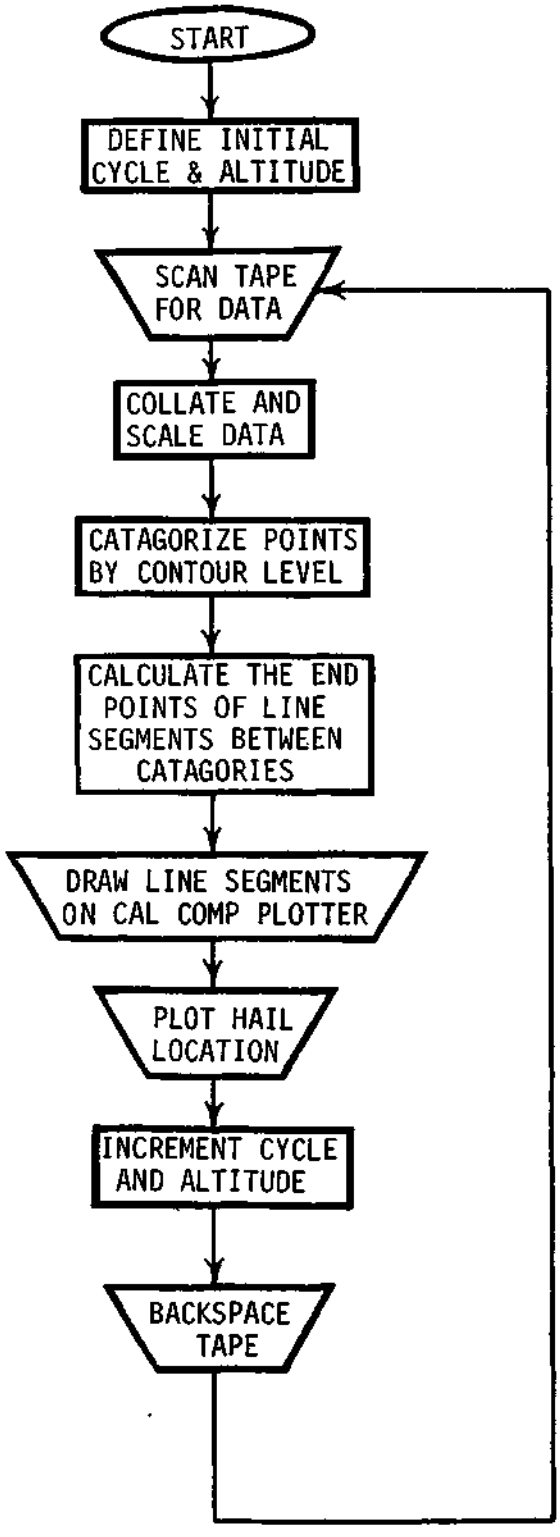

ECHO VOLUME-GRADIENT ANALYSIS PROGRAM

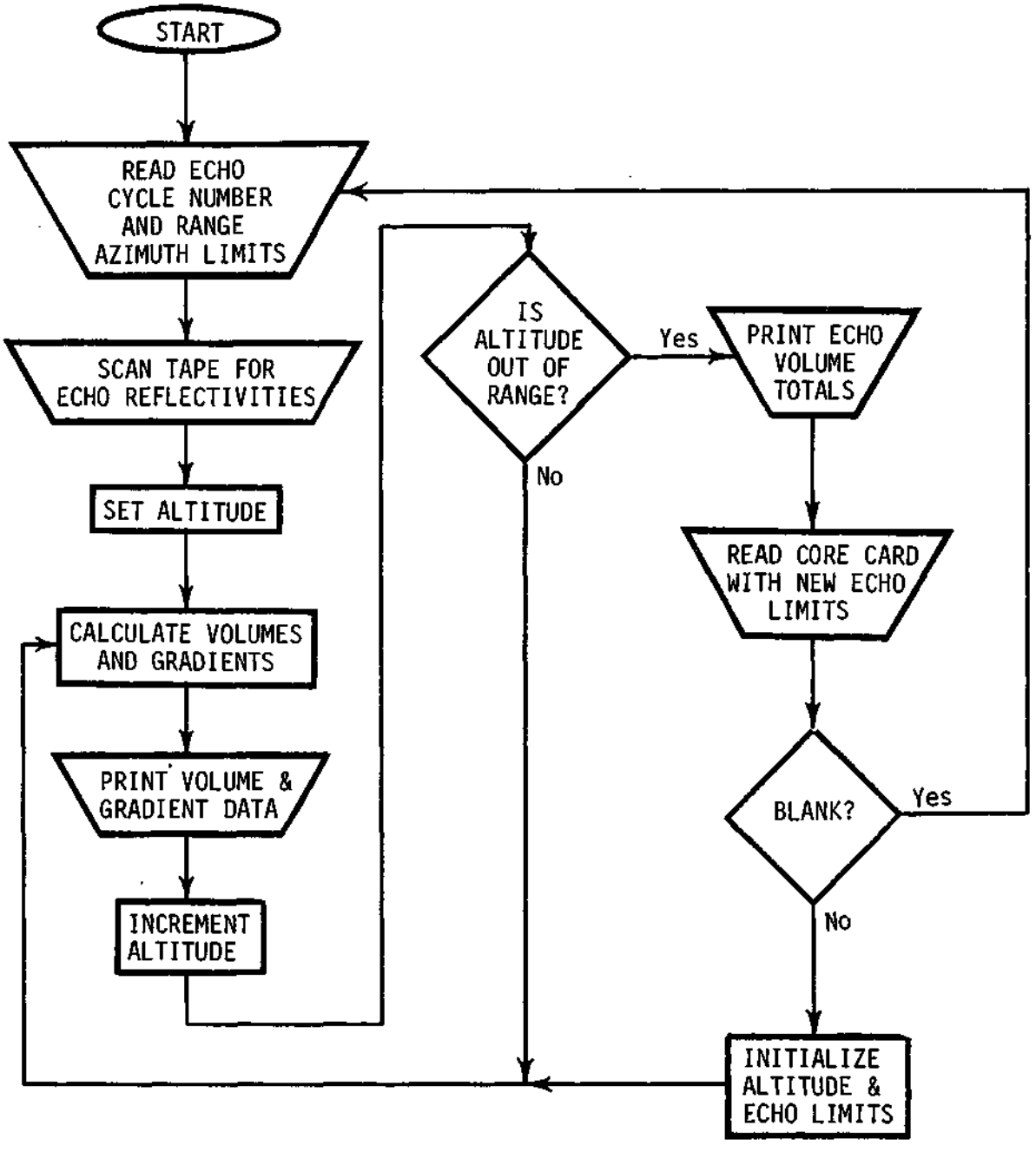

After a study of the CAPPI maps prepared by the echo plot program, the user specifies the range and azimuth limits of echoes selected for analysis. The echo tape is scanned and a three dimensional reflectivity array is constructed within the memory of the computer. Echoes or portions of echoes can be eliminated by specifying their range and azimuth limits, if desired.

Reflectivity area values are printed for each specified height level, and a reflectivity-volume table is printed for the entire echo. At each specified height, gradients are also calculated from the computed centroid of the highest reflectivity area in eight directions based on reflectivity values at each 1/2 mile intervals. Tables of these gradients are printed along with tables of average reflectivity values for all directions at designated distances from the centroid.

Additional instructions allow the same analyses to be preformed on individual cores within the larger echo. These are also defined from the CAPPI maps.